628.53
W811r
#10

Voget
Dailey

AIR POLLUTION ANALYSIS LABORATORY **** APAL REPORT #10

DETECTION OF PARTICULATE AIR POLLUTION PLUMES FROM MAJOR POINT SOURCES USING ERTS-I IMAGERY

by

Walter A. Lyons
Air Pollution Analysis Laboratory
College of Engineering and Applied Science
University of Wisconsin-Milwaukee

STATE WATER SURVEY DIVISION LIBRARY COPY
DEC 15 1975

and

Steven R. Pease
Department of Geography
University of Wisconsin-Milwaukee

Milwaukee, Wisconsin 53201

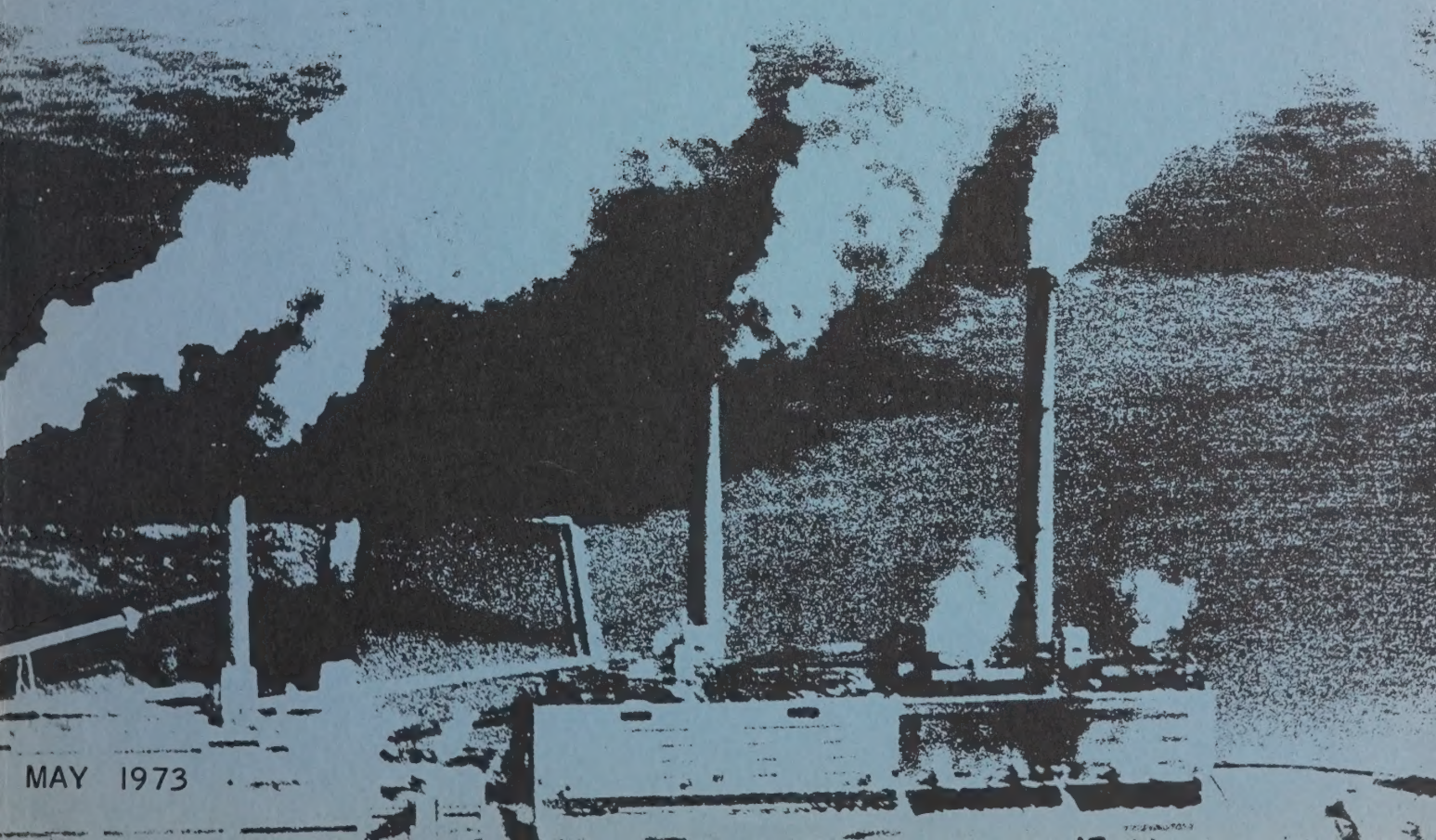

MAY 1973

[Reprinted from BULLETIN OF THE AMERICAN METEOROLOGICAL SOCIETY, Vol. 54, No. 11, November 1973, pp. 1163–1170]
Printed in U. S. A.

detection of particulate air pollution plumes from major point sources using ERTS-1 imagery[1]

Walter A. Lyons
College of Engineering and Applied Science
University of Wisconsin–Milwaukee
Milwaukee, Wis. 53201
and Steven R. Pease
Department of Geography
University of Wisconsin–Milwaukee
Milwaukee, Wis. 53201

Abstract

The Earth Resources Technology Satellite (ERTS-1) launched by NASA in July 1972 has been providing thousands of high resolution multi-spectral images of great interest to geographers, cartographers, hydrologists, agriculturists, etc. The meteorological content of these observations, however, has only been slightly realized. In particular, it has been found possible to detect the long-range (over 50-km) transport of suspected particulate plumes from the Chicago-Gary steel mill complex over Lake Michigan. The observed plumes are readily related to known steel mills, a cement plant, refineries, and fossil-fuel power plants. This has important ramifications when discussing the inter-regional transport of atmospheric pollutants, in this case from the Chicago Interstate to the Southeast Wisconsin Air Quality Control Region. Analysis reveals that the Multispectral Scanner Band 5 (0.6–0.7 μm) provides the best overall contrast between the smoke and the underlying water surface.

1. Introduction

The Federal Clean Air Act of 1967 (amended 1970) divided the United States into Air Quality Control Regions (AQCR). The boundaries of these regions were ideally to be chosen to delineate independent self-contained "air sheds" where air quality levels would be determined by dispersion from sources within that region. The actual boundaries selected often were compromises between meteorological and political realities. An AQCR's final compliance with national Air Quality Standards is ultimately dependent upon the successful formulation and implementation by regional authorities of the necessary emission control strategy for sources within that region. In reality, however, two adjacent AQCR's might occasionally find themselves breathing each other's effluents due to long-range inter-regional transport of pollutants. A case in point is the Southeast Wisconsin AQCR (the seven counties of southeastern Wisconsin, including metropolitan Milwaukee) and the Chicago Interstate AQCR (northeast Illinois and the two northwesternmost counties of Indiana). In the latter, there exist numerous extremely large point sources, especially of suspended particulates from steel mills, fossil-fuel power plants, refineries, and cement operations. The evidence has gradually been accumulating that these sources are indeed more than just local problems.

In August 1967, the principal author participated in a flight of an NCAR Queen Air, instrumented to monitor ice nuclei (Langer, Biter, and Dascher, 1968). The object of the study was the dispersion of anthropogenic ice nuclei emanating from the Chicago-Gary steel mill complex. Under conditions of brisk southwesterly flow over southern Lake Michigan, with a rather strong synoptic-scale capping subsidence inversion around 1300 m, a clearly defined plume of ice nuclei was easily tracked to the vicinity of Battle Creek, Mich. (some 170 km downwind). More recently, on a spring day with south-southeast flow up the lake, elevated layers of red iron-oxide smoke were seen drifting past Milwaukee (Fig. 1). Again the most likely origin of this smoke was the mills at the southern end of the lake—160 km away.

The effect of the much larger Chicago Interstate AQCR is probably significant, but most difficult to ascertain qualitatively. It has been estimated that approximately 10% of the suspended particulates measured in

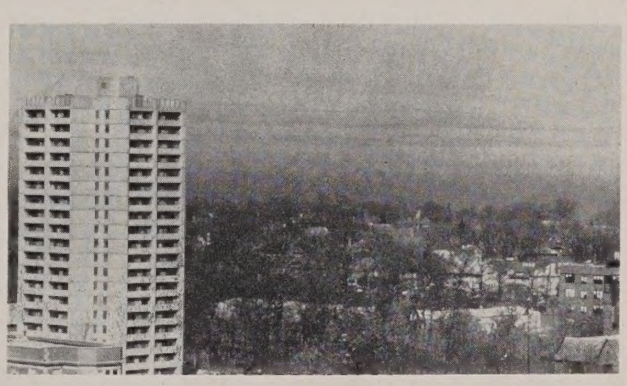

FIG. 1. Photograph, looking east, from University of Milwaukee–Wisconsin campus, showing layers of iron oxide red smoke over Lake Michigan, during brisk south-southeast winds and very stable conditions in March 1973. The source of the smoke is presumably the Chicago-Gary area.

[1] This paper is Report No. 10, Air Pollution Analysis Laboratory, University of Wisconsin–Milwaukee.

FIG. 2. Smoke plume from large fossil fuel power plant located south of Milwaukee's Mitchell Airport (MKE). This plume, photographed looking north from an NCAR Queen Air on 22 August 1968, was advecting over a relatively cold lake. The air was so stable that the plume could be seen extending for over 100 km to the east.

the Milwaukee area originate in and around Chicago.[2] Frequently in Milwaukee, several hours after the surface winds shift to the south or southeast, there is a rapid increase in haze and smoke, presumably the influence of inter-regional transport from the Chicago area. Certainly in any megalopolis, such as found along the East and West Coasts, adjacent AQCR's would indeed be expected to be exchanging pollutants.

In the emerging Great Lakes megalopolis, which shows signs of extending from Green Bay, Wis., to Buffalo, N.Y., in the not-too-distant future, the peculiar meteorological effects of the Great Lakes often exacerbate this inter-regional transport. When continental air masses advect across the relatively warm lakes in winter, any plume moving over a Great Lake will be rapidly dispersed. Turbulence generated by the free convection rising from the surface can be extreme, sometimes to the point of generating a myriad of miniature waterspouts or "steam devils" (Lyons and Pease, 1972). Thus, if plumes from northern Indiana are to pass over Lake Michigan to southwestern Michigan or Wisconsin, they probably arrive diluted to an extreme degree. From early spring through late summer, quite the opposite situation prevails; air temperatures frequently exceed those of the lake by 10, 20, or sometimes 30C. Extremely intense, though shallow (100–200 m) surface conduction inversions form over the lake (Lyons, 1970). Air streams advecting over cold lakes not only are rapidly cooled in their lowest layers, but due to the absence of upward convective heat transport do not warm and destabilize in the overlying layers, as they do over land during the day. The almost total lack of cumulus clouds over the Great Lakes on summer afternoons is one manifestation of this stabilizing process (Lyons, 1966). A plume from a large elevated point source such as a steel mill or power plant may travel for long distances over water with relatively little dilution and arrive on a downwind shoreline in still very high concentrations. Fig. 2, a plume from a large fossil fuel power plant south of Milwaukee, dramatically illustrates the point.[3] This plume could be seen extending over 100 km to the east with minimal dispersion evident. If such a plume arrives on a downwind shore during mid-day and insolation is sufficient, it is fumigated to the surface after a few kilometers of inland travel (Lyons and Cole, 1973) and may cause high pollution levels, the origin of which could be quite baffling to local control officials.

That there is inter-regional pollution transport in the vicinity of the Great Lakes is clear, but measurement of actual amounts is a problem. Until recently, reliable instruments for measuring total suspended particulate matter using an aircraft in real time was not available. Even with technology providing the measuring device, obtaining a quasi-synoptic profile of plumes extending for at least 100 km downwind from an area as large as Chicago-Gary is both difficult and expensive, particularly if such measurements are needed on a semi-regular basis. The ideal solution would be a satellite monitoring system. Until recently no satellite was capable of such observations, but with the launching of NASA's Earth Resources Technology Satellite (ERTS-1) on 23 July 1972, the prospect has improved markedly.

2. The Earth Resources Technology Satellite

ERTS was designed specifically for environmental monitoring. It was placed in a nearly circular, 99.11 degree orbit, nominally about 915 km, with a period of 103.267 minutes. The sun-synchronous orbit has a descending node time of 0942 LST. Images are 185 by 185 km on a side. It takes 251 revolutions (18 days) to make one complete global coverage. Thus every portion of the earth (between 81° north and south latitude) is viewed at least once every 18 days. At the latitude of Chicago, there is approximately 35% horizontal image sidelap, so some locations can be seen on successive days. A one-year mission life was contemplated and, as of March 1973, more than 34,000 images had been collected. All images are characterized by a zero or near-zero zenith angle, with illumination depending on the solar elevation angle, a function of date and latitude of observation.

The two great advantages of ERTS are its extremely high resolution and a multi-spectral imaging capability. The original specifications for the multi-spectral scanner (MSS) called for 100–200 m resolution. Initial results have shown some high contrast targets as small as 50 m. Highways, airport runways, small ponds, jet contrails, harbor breakwaters, etc., are routinely visible. The four spectral bands are 1) MSS-4, 0.5–0.6 μm ("green" band);

[2] "A Statewide Implementation Plan to Achieve Air Quality Standards for Particulates, Sulfur Oxides, Nitrogen Oxides, Hydrocarbons, Oxidants, and Carbon Monoxide in the State of Wisconsin." Regulations proposed by the State of Wisconsin, Department of Natural Resources, January 1972.

[3] Subsequent to the taking of this photograph in 1971, the particulate emissions from this power plant were largely eliminated.

2) MSS-5 0.6–0.7 μm ("red" band); 3) MSS-6, 0.7–0.8 μm; and 4) MSS-7, 0.8–1.1 μm ("near infrared" band). ERTS products are available in several formats including digital tapes, 9-1/2 by 9-1/2 inch black and white and color prints and transparencies, and most routinely, 70-mm negative and positive transparencies (Mac Callum, 1973).[4]

Because the four spectral bands are viewed simultaneously in space and time, it is possible to use color-additive viewing techniques to produce color-coded results. Combining MSS bands 4, 5, and 7 results in a false-color infrared image. The red color associated with foliated vegetation makes this color analysis a valuable diagnostic tool in agriculture, forestry, and land-use studies, but for the meteorologist the ERTS multispectral imaging techniques are most useful in penetrating thick haze, revealing cloud shadows, delineating snow cover from vegetation, and demarcating land/water boundaries.

The various design characteristics prompted the UWM Air Pollution Analysis Laboratory to submit a proposal to study ERTS-1 data. Before launch, it was hoped that a satellite with these characteristics would be capable of detecting major plumes of suspended particulates, making possible synoptic studies of inter-regional pollution transport over the southern Lake Michigan basin.

3. The study area

The heart of the Chicago-Gary industrial complex stretches from the southeastern part of the City of Chicago eastwards along the shoreline of Lake and Porter Counties, Indiana, to the east of Gary. Fig. 3 is an aerial view of a part of this region, taken from an NCAR Queen Air at an altitude of about 200 m early on the morning of 15 July 1968, when brisk southwesterly flow was advecting numerous smoke plumes over the lake.

A total of 16 major particulate sources have been located in the study area (Figs. 3 and 6). The estimated annual output of particulates (provided by local air pollution control officials) and the source type are listed in Table 1. The size of some of these sources is truly remarkable. Source 3, for example, a cement plant, discharges over 140,000 tons/year of particulates. In comparison, all of Milwaukee County, Wis., a relatively industrialized area, had a 1970 suspended particulate emission of only approximately 45,000 tons/year.

4. The observation

During the morning of 1 October 1972, brisk southwest surface flow covered the southern Lake Michigan basin area (Fig. 4). A bank of altocumulus clouds, associated with a trough, was present to the north and east of the Chicago region and was moving rapidly northeastwards. A strong nocturnal radiation inversion had been present at 0600 CST according to the Peoria, Ill. (PIA) sounding (inset, Fig. 4). The synoptic situation was thus similar to that when the aircraft photographs shown in Fig. 3 was taken. Figures 5 and 6 are portions of the ERTS images taken at approximately 1003 CST.[5] They have been enlarged to show a region approximately 90 n mi wide. Figure 5, in band MSS-4, appears to be a relatively low-contrast image. Any plumes emanating from the steel complex are barely discernible, the radiance of the lake surface being so large as to be comparable to that of the smoke plumes in that portion of the spectrum. The 1000 CST airway observations are superimposed. However, in Fig. 6, band MSS-5, a number of particulate plumes can be seen streaming northeastward, disappearing beneath the altocumulus cloud deck

FIG. 3. Photograph (looking north) of a portion of the Chicago-Gary industrial complex, taken from an NCAR Queen Air, on the morning of 15 July 1968. The numbers refer to the sources listed in Table 1. ,

[4] Details on ordering ERTS products can be directed to: The EROS Data Center, U.S. Department of the Interior, Geological Survey, 10th and Dakota Aves., Sioux Falls, S.D. (605) 339-2270.

[5] NASA ERTS Image Identification Number 1070 16041.

TABLE 1. Estimated annual tonnage of suspended particulate emissions from major point sources in the Chicago Interstate Air Quality Control Regions.

No.	Type source	Emissions (tons/year)
1	Steel mill fabrication	20,394
2	Steel mill	82,474
3	Cement plant	142,675
4	Fossil fuel power plant	1,952
5	Steel complex	88,597
6	Steel complex (open burning)*	
7	Steel complex	
8	Steel complex	
9	Steel mill	24,000
10	Fossil fuel power plant	4,752
11	Steel mill/fabrication	4,000
12	Steel mill	5,900
13	Oil refinery	1,596
14	Oil refinery	1,978
15	Oil refinery	1,014
16	Steel mill	3,562

* Probably short-lived ground site.

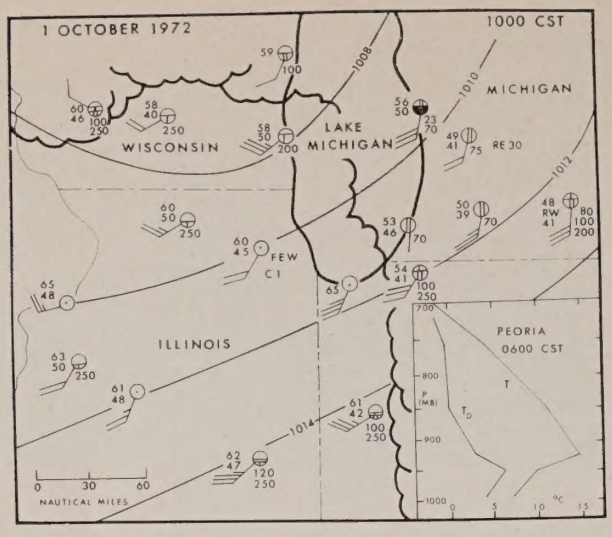

FIG. 4. Synoptic conditions, 1000 CST, 1 October 1972. An overcast area of altocumulus is present to the north and east of the study area. Isobars every 2 mb, one wind bar equals 5 kt. Inset shows 0600 CST Peoria, Ill., radiosonde.

at a distance of about 60 km. The solar elevation angle is approximately 40°.

It should be noted that due to the various degradations involved both in making the photographic print and in publication, the plumes do not appear as clear as in the original 70-mm negatives. The prints were also photographically dodged to maximize details over both land and water.

The plumes in these images, for the most part, are combinations from several point sources. The most pronounced plume, from source 8, is not exclusively from a single stack, but from an entire mill complex, with one stack dominating. The total spread of the visible plume at 60 km downwind is about 4.5 km. The plume apparently emanating from source 2 actually is the combined result of emissions from two large steel complexes (with probably 30 stacks in total) plus smaller plumes from refineries upwind from the shoreline (sources 14 and 15). The cement plant, source 4, can be seen emitting its own discrete plume; however, it is only detectable for about 10 km out over the lake. It would seem likely that, in the period just prior to ERTS's passage, it was emitting at a rate far less than its yearly average would suggest.

Measurements of plume spread can be converted into useful information regarding over-water mesoscale diffusion of pollutants. First, however, it must be determined what the visible edge of the plume represents in reality. Sometimes, the visible plume may be correlated to a parameter such as the point where concentrations drop off to 10% of the centerline value, or 2.15 σ_y, in the parlance of Pasquill (1961) and Gifford (1961). If that were the case, then this plume would appear to have a diffusion rate characteristic of Class E (rather stable atmosphere) in the empirical classification of atmospheric stabilities used in Gaussian plume diffusion calculations. Until aircraft measurements of suspended particulates are made in conjunction with ERTS images to relate radiance to some physical parameter, the actual estimates of plume spread characteristics must remain tentative.

5. Analysis

An important consideration is the choice of the appropriate ERTS spectral band to provide optimum discrimination of a particulate plume against the underlying surface, in this case water. The plume will be most visible on the photograph when the difference between the optical density of the plume image and the optical density of the lake-surface image is greatest. Plume visibility over a water surface will thus be enhanced by: 1) decrease in the spectral albedo of the lake surface, 2) increase in overall image contrast, and 3) increase in the amount of radiation scattered and/or reflected vertically upwards from the solar beam by the plume. In the case of a plume advecting over a surface of very high spectral albedo, a fourth factor would have to be considered: the extent to which a plume attenuates solar radiation reflected vertically upwards from the surface, a factor dependent on the geometry of scattering and absorption of radiation by the plume.

The first of these major considerations, the spectral albedo of the lake surface, shows a marked variation by wavelength. Direct reflection of solar radiation from the lake surface makes a relatively minor contribution to the variation of lake albedo in the four ERTS bands. Reflection vertically upwards from the lake surface is small, of the order of 2%, and for a solar elevation angle of 40° shows only slight wavelength dependence, with very slightly higher values in the lower wavelengths of the visual spectrum (Kondratyev, 1969).

Far more important in influencing the spectral albedo of the lake is the wavelength dependence of solar radiation absorption within the lake itself. The lower the spectral absorption coefficient within the lake for any wavelength, the greater is the penetration of incident solar radiation into the lake and the greater is the likelihood of backscattering upward by water molecules and hydrosols, i.e., Rayleigh and Mie scattering respectively. For distilled water, maximum transmissivity occurs at 0.46 μm, and absorption increases rapidly with increasing wavelength, resulting in a darker lake image. As an example, the mean absorption coefficient for pure water in ERTS band MSS-4 is approximately six times less than the coefficient for MSS-5, and the lake thus should appear brighter. Increased amounts of suspended and dissolved matter shift the wavelength of minimum absorption and maximum lake albedo to longer wavelengths. According to Kondratyev (1969), sea water (and lake water?) typically has minimum absorption near 0.55 μm, which is the center of ERTS band MSS-4.

An additional consequence of the greater transparency of water in the blue and green portion of the spectrum occurs in the case of shallow water, where reflection from

the lake bottom may further increase values of surface lake albedo and limit the ability to detect pollution plumes near shore.

Another important factor influencing lake spectral albedo is the variation by wavelength of scattering geometry beneath the lake surface. As Rayleigh scattering has more pronounced backscatter than Mie scattering, increased Rayleigh scattering will produce higher values of lake spectral albedo. In the blue portion of the spectrum, about 40% of all scattering within the lake is Rayleigh scattering by water molecules. In contrast, at the center of band MSS-5 (0.65 μm), only about one in every 35 scattering events is typically molecular Rayleigh scattering (Plass and Kattawar, 1969); the rest are strongly forward-scattering Mie scattering events produced by hydrosols. This, coupled with the higher absorption coefficients at longer wavelengths, produces a much darker lake image in band 5 than in band 4. In fact, in the near infrared (MSS-7), water surfaces appear black, the result of very high absorption coefficients of the lake water and the very low amounts of Rayleigh backscattering at long wavelengths.

All other factors constant, a higher value of lake spectral albedo will produce a higher value of upward hemispheric radiant flux. The surface albedo is a measurement of the ratio of radiation reflected or scattered upwards in all directions, i.e., upward hemispheric radiant flux immediately above the surface, to incident downward hemispheric flux. The very narrow scan angle of the ERTS scanner, however, intercepts only that portion of the total flux that is directed vertically upwards. Spectral variations in directional radiation intensity (radiance) in the upward vertical direction may exceed spectral variations in the total hemispheric radiant flux which is produced by difference in lake spectral albedo, including reflection in all directions. In a theoretical study by Plass and Kattawar (1969) of the angular distribution of the radiance over an ocean surface, it was found that for a solar beam incident angle near 40% (as in the present study) and a wavelength of 0.65 μm (MSS-5), a pronounced minimum of upward radiance in the vertical direction occurs which is an order of magnitude smaller than maximum values found near the horizon. For shorter wavelengths, however, upward radiance is distributed much more uniformly over all zenith angles, and the radiance value in the vertical direction is several times greater than at 0.65 μm. If a similar qualitative relationship holds over a turbid lake, then the greater angular variations of radiance at longer wavelengths would further accentuate differences in spectral albedo to produce darker lake images with increasing wavelength.

The second major consideration limiting our ability to detect particulate plumes against an underlying surface is reduction of overall image contrast. Atmospheric Rayleigh scattering and Mie scattering from haze or pollution layers generally act to increase overall radiance. Because image density of a positive transparency ideally is inversely proportional to the logarithm of exposure and hence, in the case of ERTS imagery, to the logarithm of the radiance, a given increase in radiance due to atmospheric scattering will produce a greater decrease in image density for a low radiance target than for a high radiance target. As a result, the photographic image of a low-albedo target such as a lake shows a greater increase in brightness due to atmospheric scattering than does a highly reflective target such as a cloud or pollution plume, and overall image contrast is reduced. Because scattering varies with wavelength, maximum inherent image contrast (defined for convenience as the difference in photographic density between a target having an albedo equal to unity and a target with zero albedo), will also show variation between spectral bands.

Greatest variation of maximum inherent image contrast between ERTS spectral bands occurs as a result of sky luminance produced by Rayleigh scattering. Although Rayleigh scattering is most pronounced at the short-wavelength end of the visual spectrum, the average Rayleigh scattering coefficient in ERTS band MSS-4 (0.5 to 0.6 μm) is still relatively high, amounting to 45% of the coefficient for 0.4 to 0.5 μm (Kondratyev, 1969), but decreases rapidly for longer wavelengths. The spectral variation of Mie scattering by atmospheric aerosols is much less than for Rayleigh scattering and is marked by gradual decline with increasing wavelength. Computer simulation models of Rayleigh and Mie scattering in a normally hazy atmosphere (Plass and Kattawar, 1968) indicate that maximum inherent image contrast (as defined above) may be over twice as great at 0.7 μm as at 0.4 μm, and maximum inherent image contrast is even greater in the near infrared. Increasing aerosol content increases the contribution of Mie scattering, produces a more uniform distribution of radiance over all zenith angles (i.e., more isotropic), and increases values of upward radiance in the vertical direction. The resulting reduction of image contrast with increase in aerosol content occurs for all wavelengths, but is most pronounced for shorter wavelengths of the solar spectrum (Plass and Kattawar, 1970).

The combined effects of high lake spectral albedo and low inherent image contrast can be seen by examining Fig. 5. Although urban features of the Chicago-Gary area, regions of high turbidity in Lake Michigan, and the deck of altocumulus to the northeast are readily visible, plumes advecting over the lake from Gary and Chicago are virtually undetectable at distances exceeding 5 to 10 km downstream from the lakeshore because of the bright lake and reduced image contrast. Attempts to enhance contrast photographically through dodging and use of high contrast paper rendered plumes visible only very near shore where particulate concentrations were highest.

From the above discussion, it might be expected that the optimum spectral band for plume tracking over a lake, in the absence of ice cover, would fall in the near-

FIG. 5. ERTS-1 image, MSS-4 (0.5–0.6 μm) taken at 1003 CST, 1 October 1972. Aviation weather observations superimposed.

infrared range. For band MSS-7 (0.8 to 1.1 μm), sky luminance is negligible, and a high absorption coefficient for the lake water produces very low spectral albedo values and a very dark lake image on a positive photograph. For liquid-water clouds, whose albedo is practically independent of wavelength up to 1.3 μm (Kondratyev, 1969), band MSS-7 does indeed provide maximum contrast in image density between cloud and lake. Such does not seem to be the case for particulate plumes, however, because of a third major consideration: the spectral variations in albedo of a dense particulate plume. Data on the geometry of multiple scattering and diffuse reflection from pollution plumes are limited. However, tables of primary Mie scattering (deBary *et al.*, 1965) indicate a dependence of angular scattering intensities on wavelength, as mentioned above. For the present case, considering scattering vertically upwards from a solar beam with an elevation angle of 40°, primary scattering coefficients in the near-infrared (1.0 μm) are only 45 to 75% of the values at the center of the green band (0.65 μm). Furthermore, computer simulation models of short-wave radiative transfer in a highly turbid aerosol layer (Plass and Kattawar, 1972) show higher values of upward radiance (measured at the top of the atmosphere) at 0.7 μm than at 0.9 μm (within band MSS-7) for all zenith angles. If the same qualitative relationship holds in the case of multiple scattering in a highly turbid particulate plume, then maximum inherent brightness should occur in the lowest visual wavelengths rather than in the near infrared.

Thus, from various theoretical considerations it would appear that the poorest plume discrimination above a water surface would be in the shortest wavelengths, as confirmed by MSS-4 (Fig. 5). On the other hand, while it was initially expected that the near-infrared (band 7) would optimize plume contrast over water, as is the case

with liquid-water clouds, the higher inherent brightness of plumes in the visible spectrum results in the "red" band being the best for smoke detection. The plumes were visible in bands MSS-6 and 7; band 5, however, provided the best compromise between the high lake spectral albedo and low contrast of the shorter wavelengths and the diminished plume albedo in the longer wavelengths.

6. Conclusions and future research

From this case study, it now appears highly likely that when the proper meteorological conditions (south-southeasterly winds) coincide with an ERTS passage, we will be able to detect major air pollution plumes entering the Southeast Wisconsin "airshed" from sources over 100 km removed. If it can be shown that this interregional pollution transport contributes significantly to the observed particulate levels in the Milwaukee area, a most interesting question will arise. If Southeast Wisconsin fails to reach its air quality standards for suspended particulates, should it be penalized for the "sins of emission" of other regions?

While ERTS images such as the ones discussed are of great interest in themselves, their value is somewhat limited by the unavailability of actual "ground truth" supporting data. UWM's Air Pollution Analysis Laboratory has now instrumented a Cessna 336 aircraft with an array of air pollution and meteorological sensors. Included are fast response devices for monitoring total suspended particulate mass loadings and particle concentrations in several size ranges. Onboard processing and tape data logging will make it possible to fly repeated profiles of selected plumes coincident with ERTS. Thus it may be possible to determine radiance/mass

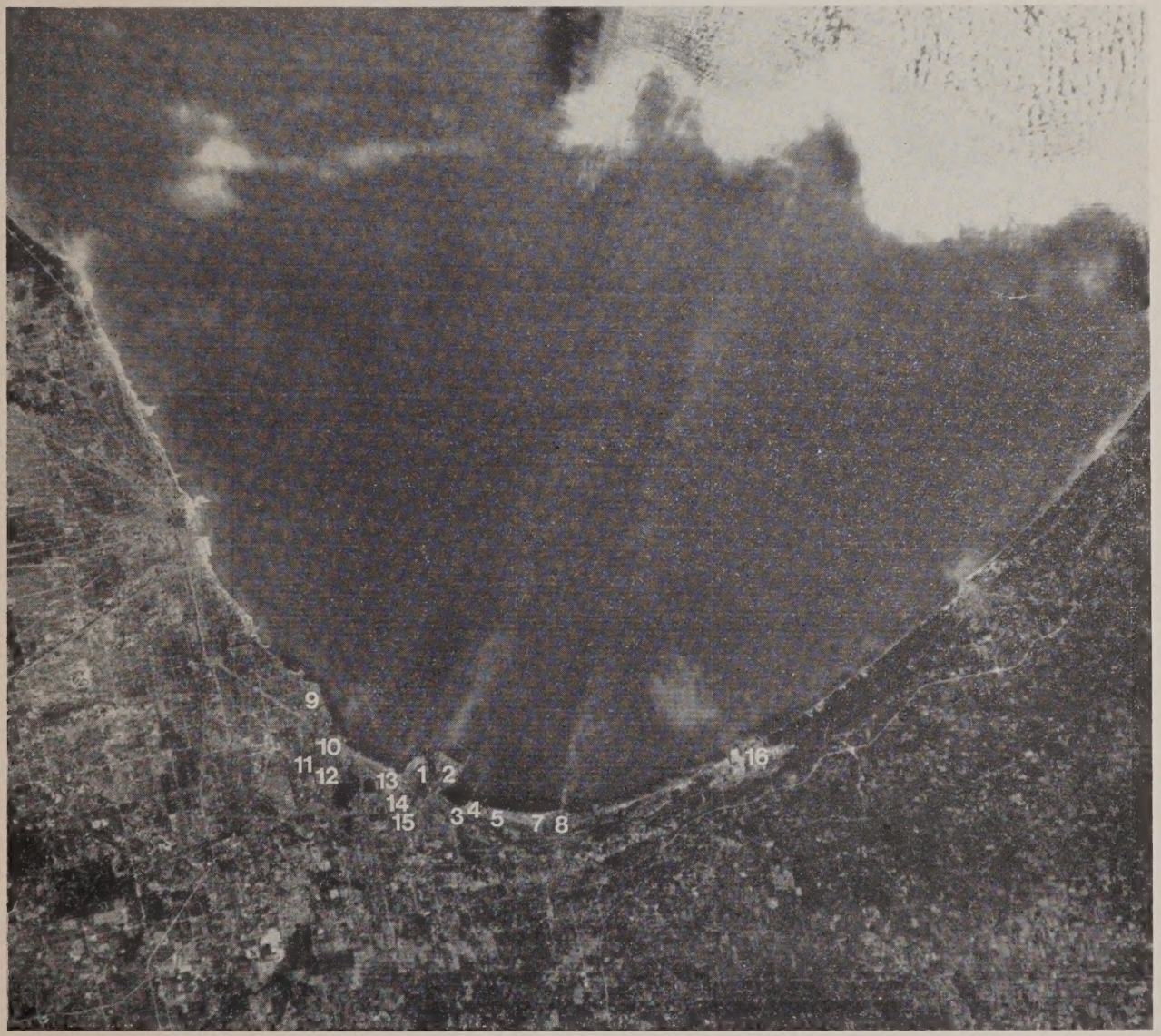

FIG. 6. ERTS-1 image, MSS-5 (0.6–0.7 μm). Smoke plumes clearly visible. Numbers refer to sources listed in Table 1. Altocumulus clouds are visible to northeast. Patches of cirrus and near shore water sediments can also be noted.

loading relationships, and also to ascertain how well the actual plume conforms to the Gaussian profile so often imposed in numerical studies. Densitometric analysis of ERTS negatives would also accompany such studies.

Unless they are unusually dense, smoke plumes are harder to detect over land than over water. Land surfaces are generally much brighter than water and exhibit marked spatial and seasonal variations in radiance. Using false-color infrared, at least during summer, seems to be reasonably successful at times, but visual detection of many plumes may not be routinely possible. The next analysis step then should be smoke detection by computerized pattern recognition techniques employing the primary ERTS digital tape data rather than photographically reconstructed products.

Acknowledgments. We would like to thank Prof. Robert W. Pease, Department of Geography, University of California-Riverside, who kindly provided numerous color-combined photographs of the scenes used in this study, as well as others. The considerable photographic darkroom expertise of Mr. Peter Tolsma III is gratefully acknowledged. Dr. Paul Harrison, Chicago Department of Environmental Control, most graciously provided the emission inventory of the sources studied. This work was partially supported by the National Aeronautics and Space Administration (Contract NAS5-21736), the U.S. Environmental Protection Agency (Grant No. R800873), and the State of Wisconsin Department of Natural Resources. This paper is also Contribution No. 85, Center for Great Lakes Studies, University of Wisconsin-Milwaukee.

References

deBary, E., B. Braun, and K. Bullrich, 1965: Tables related to light scattering in a turbid atmosphere, Vol. I. *Air Force Cambridge Research Laboratories Special Report No. 33*, Bedford, Mass.

Gifford, F. A., 1961: Uses of routine meteorological observations for estimating atmospheric dispersion. *Nucl. Safety*, **2**, 47–51.

Kondratyev, K. Ya., 1969: *Radiation in the Atmosphere*. New York, Academic Press, 912 pp.

Langer, G., C. Biter, and A. Dascher, 1968: An automated aircraft instrumentation system for cloud nucleation studies. *Bull. Amer. Meteor. Soc.*, **49**, 914–917.

Lyons, W. A., 1966: Some effects of Lake Michigan upon squall lines and summertime convection. *Proc. 9th Conf. Great Lakes Res., Intl. Assoc. for Great Lakes Res.*, Ann Arbor, Mich., 259–273.

——, 1970: Numerical simulation of Great Lakes summertime conduction inversions. *Proc. 13th Conf. Great Lakes Res., Intl. Assoc. for Great Lakes Res.*, Ann Arbor, Mich., 369–387.

——, and S. R. Pease, 1972: "Steam Devils" over Lake Michigan during a January arctic outbreak. *Mon. Wea. Rev.*, **100**, 235–237.

——, and H. S. Cole, 1973: Fumigation and plume trapping on the shores of the Great Lakes during stable onshore flow. *J. Appl. Meteor.*, **12**, 494–510.

Mac Callum, D. H., 1973: Availability of ERTS-1 data. *Bull. Amer. Meteor. Soc.*, **54**, 112–114.

Pasquill, F., 1961: The estimation of the dispersion of windborne material. *Meteor. Mag.*, **90**, 33–46.

Plass, G. N., and G. W. Kattawar, 1968: Calculations of reflected and transmitted radiance for earth's atmosphere. *Appl. Opt.*, **7**, 1129–1135.

——, and ——, 1969: Radiative transfer in an atmosphere-ocean system. *Appl. Opt.*, **8**, 455–466.

——, and ——, 1970: Polarization of the radiation reflected and transmitted by the earth's atmosphere. *Appl. Opt.*, **9**, 1122–1130.

——, and ——, 1972: Effect of aerosol variation on radiance in the earth's atmosphere-ocean system. *Appl. Opt.*, **11**, 1598–1604.

UNIVERSITY OF ILLINOIS-URBANA
3 0112 109113024